Published in IET Microwaves, Antennas & Propagation
Received on 16th December 2009
Revised on 28th September 2010
doi: 10.1049/iet-map.2009.0622

ISSN 1751-8725

Analysis of channel capacity for fixed broadband multimedia systems at 40 GHz

A.V. Alejos M.G. Sanchez I. Cuiñas

Department of Signal and Communications Theory, University of Vigo, Maxwell Street, E36310 Vigo, Spain
E-mail: analejos@uvigo.es

Abstract: The results of a wideband radio channel sounding campaign performed at 40 GHz band are presented. We have used a sounder based on the correlation of pseudorandom *m*-sequences, but some novelties have been introduced in the classical scheme of this kind of sounders. Different antenna patterns and polarisations have been combined with three groups of actual environments (indoor, outdoor and indoor–outdoor) in order to achieve general conclusions, valid for a wide range of different situations. An expression relating two of the main parameters of the wideband radio channel (coherence bandwidth and delay spread) is fitted to the measured results. The experimental data as well as this expression verify Fleury's limit, a restriction that has been extended here to define a complete region of valid values. Finally, a theoretical analysis of the channel capacity is conducted. We have stated the theoretical improvement that the channel capacity would experience owing to the use of spatial diversity or multicarrier modulations. The outcomes provide a timely insight into the expectations for the use of high data rate applications in this frequency band even in indoor conditions.

1 Introduction

Broadcast services with enhanced capabilities constitute the next generation of wireless broadband multimedia services. The millimetre wavelength band appears to be the best choice for these communication systems because of the high data rates offered and the amount of available frequency space. In the 1990s, there was growing interest in developing a new generation of fixed broadband services and the consequent deliberations about the spectrum frequency allocation and implementation issues resulted in a number of technical reports and projects [1–3], expertise work groups and research papers [4, 5]. The final phase of this extensive research activity was a set of standardisation documents and technical recommendations [6, 7] that recognise the potential that could be derived from the use of millimetre frequency bands to provide broadband telecommunication services.

Fixed systems for point-to-multipoint (P-MP) radio access constitute a fast and flexible mean compared to cable-based solutions, of offering a range of broadband digital services, especially over the last mile. In Europe the 40 and 60 GHz bands have been allocated to these broadband radio access systems. In our work, we have paid special interest to the performance characteristics of the multimedia wireless system (MWS) that will allow the deployment of fixed broadband wireless access to provide P-MP broadband digital services up to 155 Mbps [6–9].

The MWS system operating on the 40 GHz band offers a bandwidth of up to 4 GHz with the possibility of frequency reuse by means of dual polarisation. Operators will require local licences that will provide around 500 MHz of spectrum each.

Notwithstanding the possibilities offered by this band, it is not extensively used in Europe. Firstly, only a few examples of practical systems implemented in the 40 GHz band can be found, and the literature related to wideband characterisation in this band is scarce and incomplete. The initial interest in this promising band disappeared and was sidelined by the emerging wireless communications networks operating at 2.4/5.8 and at 60 GHz, mainly due to their unlicenced feature. Another cause of this lack of knowledge can be found in a radiofrequency electronics industry not so far and wide developed to allow low cost production that is readily available for lower frequencies including 28 GHz (Local Multipoint Distribution Service, LMDS).

In recent years, however, new technologies, such as the application of MIMO or diversity techniques have appeared that can increase dramatically the capacity, as we will demonstrate theoretically. The use of orthogonal frequency division multiplexing (OFDM) modulation, which has not been widely considered before in most of the references, is also contemplated here.

The objective of the measurements presented in this paper is to demonstrate the theoretical channel capacity of the 40 GHz band estimated from actual wideband radio channel parameters. A precise knowledge of multipath behaviour is a basic step to measure the degradation of the quality of service suffered by large bandwidth systems in this band. A measurement system based on the swept-time delay cross correlation (STDCC) scheme was implemented to achieve this purpose.

The propagation of signals in the 40 GHz band is influenced by the scenario where it takes place. Phenomena such as multipath, reflection, diffraction and scattering are

highly site specific [10]. The millimetre wave radio channel characteristics also depend on the pattern and polarisation of the antennas used. As a result, different environments have been chosen, as well as different antenna patterns and polarisations in order to obtain general conclusions valid for a wide range of different situations.

The main channel parameters, namely delay spread τ_{rms} and coherence bandwidth (CB), are related theoretically by an inverse dependence [11]. However, an exact and generalised expression involving τ_{rms} and CB does not exist, and must be derived from signal analysis applied to actual measurements carried out in particular channels and frequency bands.

Several approaches have been described for this relation in the literature [12–14], but many of them do not meet the restriction known as Fleury's limit [15]. It consists of a restriction to be satisfied by the values of RMS delay spread and CB. This simple bound is valid to assess whether these values have not been correctly measured.

In Section 2, we describe the hardware system used for the measurements. The selected environments are also discussed in this section. Experimental results are presented and discussed in Section 3. We propose an expression for an approximate relation between delay spread and CB in Section 4. The expression will take into account factors as polarisation, scenario (indoor, outdoor, indoor–outdoor) and correlation level. In Section 5, we offer a theoretical estimation of the channel capacity taking into account the measured parameters.

2 Measurement setup

In this section we describe the radio channel sounder implemented to drive the measurement experiments. The selected environments are also introduced.

2.1 Measurement system and procedure

An STDCC sounder was built [16]. This type of sounder transmits a PRBS sequence with a chip rate of 12.5 ns and length $M = 2^{13}-1$ bits. The power delivered to the transmitter antenna was +25 dBm. The spatial resolution of the sounder is 3.75 m, with a maximum discernible delay equal to 102.39 μs. This sounder is based on the sliding correlation technique. However, we have introduced changes to the classical configuration given in [16] to improve the performance of the sounder. The main novelty is the suppression of the sliding factor, by clocking transmitter and receiver PN sequences to the same rate. Another important change is the implementation of the receiver based on two down conversions to intermediate frequencies. The final down conversion to complex baseband is achieved by a digital off-line process. The block diagram of the sounder is shown in Fig. 1.

The measurement system was completed with a 2.4 m-long linear positioning system. It is provided with a step-by-step motor controlled from a computer embedded in the digital oscilloscope. The receiver antenna is moved horizontally, in $\lambda/8$ increments, along 400 positions.

2.2 Measurement environments

Different scenarios have been chosen to obtain results for a variety of multipath situations. They can all be grouped in three types that are listed and described below:

1. *Outdoor–outdoor environments:* Here, the MWS/MVDS are deployed in outdoor scenarios under line-of-sight (LOS) conditions. This group of environments comprises three outdoor scenarios. The receiver stays always at the same position but the orientation can be modified. Three wide terraces located at three different buildings within our university's campus were selected to place the transmitter. The terraces are similar, with concrete floors and walls. The separation distances between transmitter and receiver were about 15, 79 and 141 m. The chosen transmitter and receiver locations provide LOS links, except for the medium-distance case where vegetation in the form of a

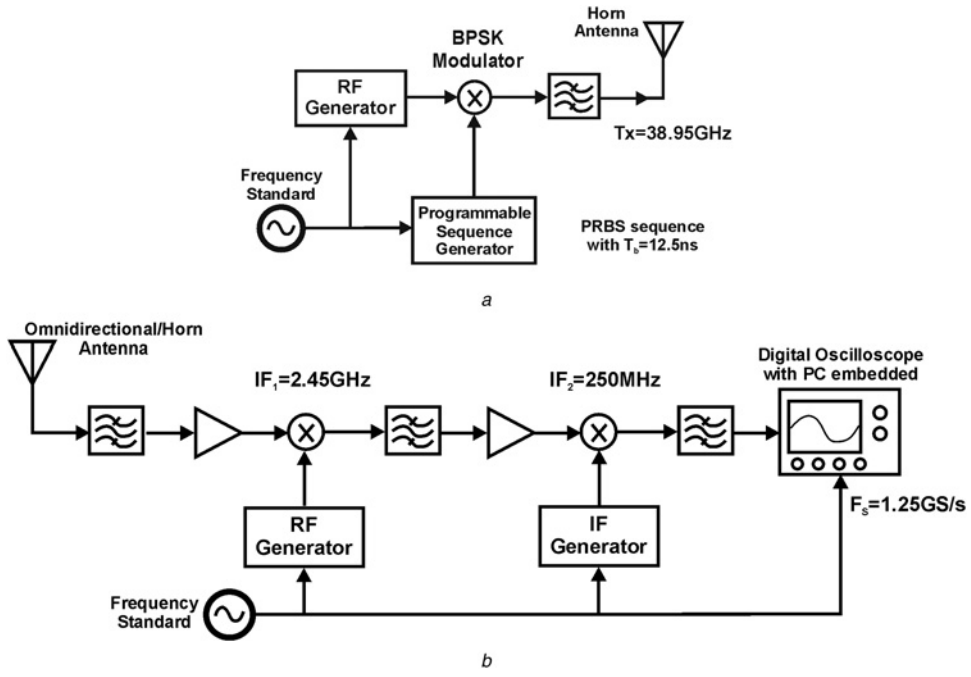

Fig. 1 *Block diagrams of*

a Transmitter
b Receiver

doi: 10.1049/iet-map.2009.0622

mass of trees with medium height and foliage can be found between both ends of the sounder. For this link, the first Fresnel ellipsoid remains unobstructed. A plan of the area in which outdoor measurements were taken is shown in Fig. 2, indicating terrace locations as well as transmitter and receiver placements.

2. *Indoor–indoor environments:* The objective here is to study the propagation inside buildings as a possible new scenario for MWS/MVDS applications. This group of environments comprises two indoor scenarios: a rectangular classroom and a conference room. For the first scenario, the walls are made of brick and there are windows along three side walls. The only furniture is several rows of wooden desks. For the second scenario, the walls are completely covered with cork except for two wooden doors. The furniture consists of several rows of stalls. In both scenarios, the distance between transmitter and receiver was 13.5 m and the antenna height was 1.52 m. The antenna heights and positions provide a LOS link with no obstructions in the first Fresnel zone.

3. *Outdoor–indoor environments:* The multipath propagation phenomenon makes the transmission possible even if there is no direct path between the transmitter and receiver [9, 17, 18]. In order to analyse this worst case, a scenario was chosen to study non-line of sight (NLOS) propagation from an outdoor location to an indoor room. This environment comprises only one scenario. The transmitter was placed on an outdoor terrace and the receiver in the adjacent laboratory. Between both ends of the sounder, the main obstacles were a concrete wall with mortar, and a glass door with a metallic frame. The distance between transmitter and receiver was 11.6 m. The height of the transmitter and receiver antennas was 1.52 m.

2.3 Measurement configurations

The combination of antennas chosen for the transmitter and receiver ends defines two configurations, one directive and another omnidirectional. The directive variant includes the option of two polarisations, so that the transmission was performed in the vertical and horizontal polarisations, with reception in the same polarisation. This also occurs with the omnidirectional variant. Directive antennas consisted of 20 dBi gain standard pyramidal horns with a beamwidth of 20°. The omnidirectional antenna used presents a gain lower than 2 dBi with an omnidirectional pattern for vertical polarisation and a directive pattern with a 60° beamwidth for horizontal polarisation.

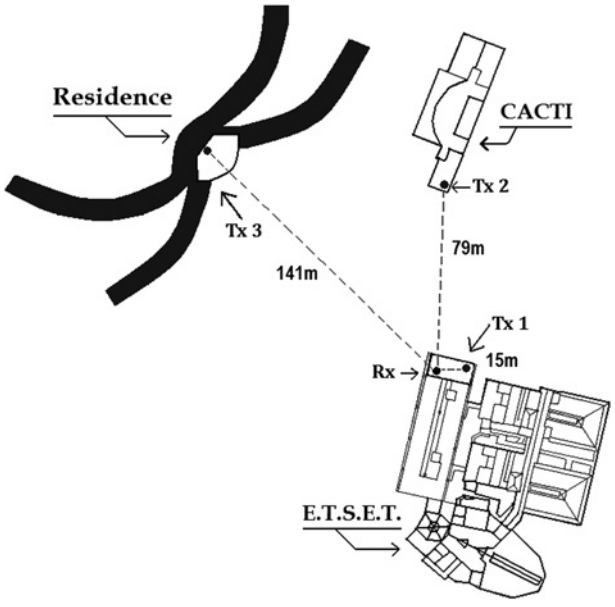

Fig. 2 *Plan of the area for outdoor measurements*

According to the link budget, for a directive configuration, the maximum allowed separation distance to surpass the sensitivity of the sounder is about 1938 m in the vertical polarisation case and 1727 m for horizontal polarisation. When the omnidirectional pattern is used, the maximum distance decreases considerably up to 194 m, for both polarisations. Otherwise, these maximum distances are larger than those used in the links of the measurement campaign presented here.

3 Experimental results

Once measurement data are obtained, they are processed to estimate the main channel functions, such as the impulse response, $h(t, \tau)$, the averaged power delay profile, $P_h(\tau)$ $o < |h(\tau)|^2 >$ and the frequency correlation function, $R_h(f)$ [11, 19]. We assumed an ergodic behaviour of the channel. The results are shown in the form of time and frequency channel parameters. These parameters are the delay spread or rms delay, τ_{rms}, and the CB.

3.1 Channel parameters

The values of delay spread and CB for each environment resulting from the measurements are summarised in Tables 1–4. From the results achieved for indoor environments we conclude that τ_{rms} depends slightly on room dimensions: larger dimensions provide higher τ_{rms} values. It tends to increase with increasing reflectivity of the walls; besides, it also depends on antenna directivity and polarisation.

Values obtained for the delay spread in indoor environments are in the range [21.9, 24.2] ns. These results agree with those presented in [20], where delay spread ranges from 10 to 60 ns are reported for indoor environments at 42.58 GHz when directional antennas are used. They also agree with [21], where delay spreads in the range 20–75 ns have been found at 40 GHz, using a combination of directive and omnidirectional antennas for indoor scenarios also.

In addition, delay spreads in the range 6.1–23.8 ns were reported in [22], where indoor wideband measurements were performed at 37.2 GHz with a combination of directive and omnidirectional antennas.

As might be expected, results show larger delay spread values when the omnidirectional antenna is connected to the receiver than when the directional one is used. This is owing to a large number of multipath components reaching

Table 1 Parameters for CB fitting curve

Environment	Indoor			
	Conference		Classroom	
Antenna	Horn	Omni	Horn	Omni
τ_{mean}, ns	17.3	18	17.9	19
τ_{rms}, ns	21.9	23.6	22.7	24.2
$CB_{0.9}$, MHz	8	4.1	4.6	4.2
$CB_{0.5}$, MHz	59.8	11.6	12.4	11.5

Table 2 Measured mean delay, delay spread and CB values for indoor environments

Environment	Outdoor			
	Link 1		Link 2	Link 3
Antenna	Horn	Omni	Horn	Horn
Horizontal polarisation				
τ_{mean}, ns	4.4	4.3	3.9	4
τ_{rms}, ns	6.7	6.3	5.3	5.5
$CB_{0.9}$, MHz	16.0	16.5	19.8	19.1
$CB_{0.5}$, MHz	62.9	65.4	66.2	63.6
Vertical polarisation				
τ_{mean}, ns	4.9	4.3	3.8	4
τ_{rms}, ns	7.7	6.6	5.2	5.6
$CB_{0.9}$, MHz	13.4	16.3	20.1	18.6
$CB_{0.5}$, MHz	60.2	67.2	67.7	63.7

Table 3 Measured mean delay, delay spread and CB values for outdoor environments

Environment	Outdoor–indoor	
Antenna	Horn	Omni
Horizontal polarisation		
τ_{mean}, ns	15.4	22.2
τ_{rms}, ns	23.5	33.5
$CB_{0.9}$, MHz	3.5	2.3
$CB_{0.5}$, MHz	18.7	14.9
Vertical polarisation		
τ_{mean}, ns	22.7	28
τ_{rms}, ns	33.3	41.6
$CB_{0.9}$, MHz	2.3	1.7
$CB_{0.5}$, MHz	8.8	6.4

the receiver with longer delays. The CB values estimated for the indoor cases are not negligible, being in the range [11.5, 59.8] MHz.

From results obtained for the outdoor environments we conclude that, in general, the delay spread decreases. Outdoor scenarios do not normally represent a severe multipath situation: no major reflection sources or obstructions appear in the environment if LOS conditions have been targeted.

If the transmitter and receiver antennas are aligned and a strong LOS component is present, we observe that an increment in the separation distance between transmitter and receiver yields lower values of the delay spread, τ_{rms}. This trend varies if the link is partially obstructed, as in the case of the medium-distance link. Also, τ_{rms} confirms a straightforward dependency on antenna directivity and polarisation.

The delay spread values for the outdoor scenarios were smaller than for the indoor case, within the range [5.2, 7.7] ns. These results agree with those presented in [23]. There, a delay spread range from 3.9 to 5.9 ns is reported for outdoor environments at 38 GHz, when directional antennas are used with a beamwidth of 3°. The CB values reach the largest values in the outdoor environments: [60.2, 67.7] MHz. The case of the NLOS link shows the highest delay spread values: [23.5, 41.6] ns. Owing to the obstruction, this scenario also shows the lowest values for CB: [1.7, 3.5] MHz.

For the case of outdoor–indoor environment, we detect that the delay spread tends to increase because of the blocking situation. In this NLOS case multipath contributions turn into the main propagation mechanisms that preserve the link. We also observe that the delay spread depends on antenna directivity and polarisation.

4 Relation for CB and delay spread

The theoretical value for the CB is established in [11] as the inverse of the delay spread according to (1)

$$\mathrm{CB} = \frac{1}{\tau_{\mathrm{rms}}} \tag{1}$$

However, the site-specific feature of the millimetre frequency characterisation leads us to assume that this expression will hardly be achieved under actual conditions. From the results presented in the previous section, we conclude that a relation between RMS delay spread τ_{rms} and CB should be a function of the correlation threshold c. Based on this, an expression has been evaluated following a fitting procedure for the different scenarios and polarisations. The resulting curves follow the general expression (2)

$$\mathrm{CB} = \frac{a_1 \cdot \arccos(c)}{(2\pi \cdot \tau_{\mathrm{rms}})} \tag{2}$$

where c is the correlation level and verifies $c \in [0, 1]$. The values of the parameter (a_1), resulting from fitting (2) to the measurement results in the different cases, are given in Table 5. The τ_{rms}-CB curves corresponding to each case of scenario and polarisation have been plotted in Figs. 3–5.

The CB values should meet Fleury's limit as described in [15]. The expression for this limit is (3)

$$\mathrm{CB} \geq \frac{\arccos(c)}{(2\pi \cdot \tau_{\mathrm{rms}})} \tag{3}$$

This condition is applicable both to the τ_{rms}-CB pairs from Tables 1–3 and also to the τ_{rms}-CB curves given in (2). In

Table 4 Measured mean delay, delay spread and CB values for outdoor–indoor environments

Modulations		QPSK	64-QAM	OFDM 64-QAM	
Parameters	CB, MHz	R_b, Mbps	R_b, Mbps	R_b, Mbps	N carriers
indoor	$CB_{0.9}$ [4.1, 8]	[7.1, 13.9]	[21.4, 41.7]	[24, 48]	[8, 16]
	$CB_{0.5}$ [11.5, 59.8]	[20, 104]	[60, 312]	[69, 360]	[23, 120]
outdoor	$CB_{0.9}$ [13.4, 20.1]	[23.3, 35]	[70, 104.9]	[81, 120]	[27, 40]
	$CB_{0.5}$ [60.2, 67.7]	[104.7, 117.7]	[314, 353]	[360, 405]	[120, 135]
outdoor–indoor	$CB_{0.9}$ [1.7, 3.5]	[3, 6]	[8.8, 18.2]	[9, 21]	[3, 7]
	$CB_{0.5}$ [6.4, 18.7]	[11, 32.5]	[33.4, 97.5]	[39, 111]	[13, 37]

doi: 10.1049/iet-map.2009.0622

Table 5 Ranges of bit rate estimated according Section 5

Environments	Polarisations	a_1	
		$c = 0.9$	$c = 0.5$
indoor	vertical	1423.45	1672.06
outdoor	vertical	1474.66	2361.52
	horizontal	1472.65	2276.23
outdoor–indoor	vertical	1059.91	1698.34
	horizontal	1132.61	2759.80

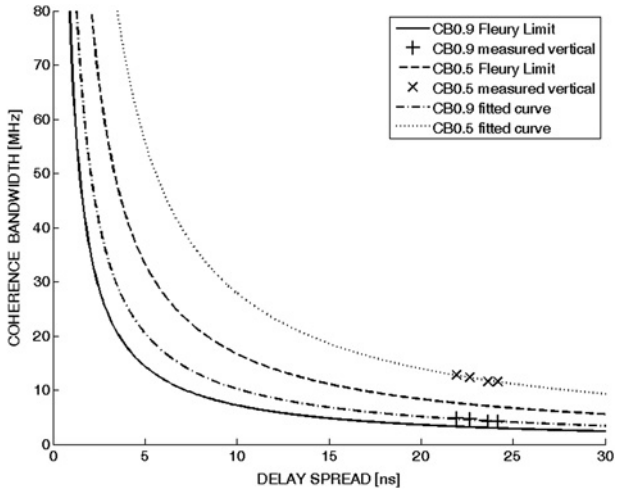

Fig. 3 *CB against delay spread for the indoor case*

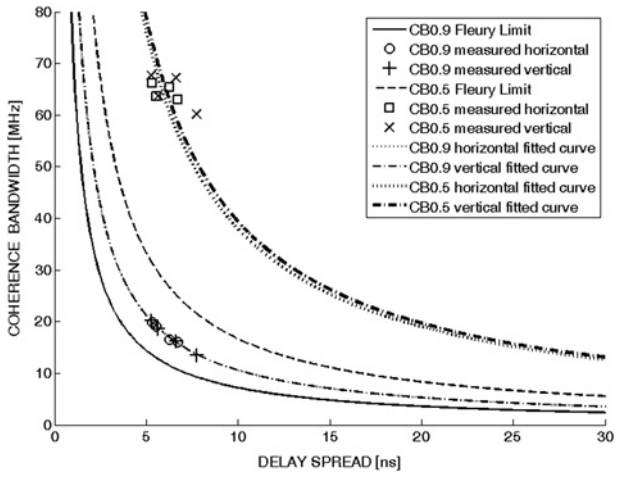

Fig. 4 *CB against delay spread for the outdoor case*

Figs. 3–5, the theoretical limit (3) has been represented for 0.5 and 0.9 correlation levels, jointly with the measured delay spread and CB values, and derived relations given by (2). As it can be seen, the results for measured CB values verify the theoretical limit given in (3). It is also noticed that all the achieved expressions (2) satisfy this restriction.

The relation given in (3) represents a lower limit for the CB values that can be obtained for a radio channel. We can also define an upper limit for the measured CB value. Taking into account (3), the maximum limit occurs when τ_{rms} tends to zero, and so CB tends to infinity. Nevertheless, for a given channel, we cannot achieve an infinite value in the CB estimation. It is obviously limited to the chip rate reverse, $1/T_c$, also called measurement bandwidth: $CB \leq 1/T_c$.

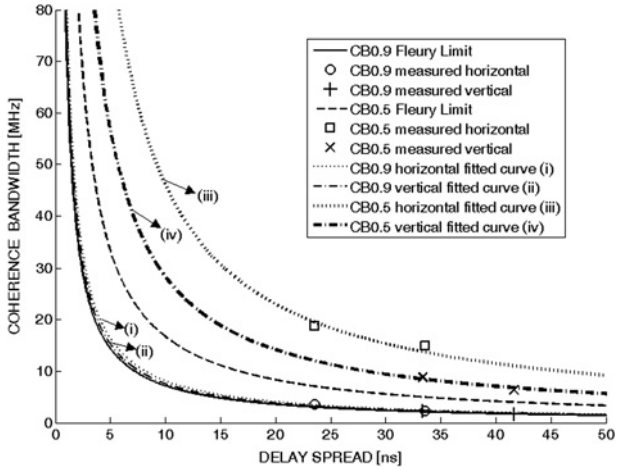

Fig. 5 *CB against delay spread for the indoor–outdoor case*

The delay spread also presents natural limits that are given by the zero delay, representing the absence of multipath, and the maximum delay measurable by the system or τ_{max}, which equals the expression $M \cdot T_c$ and depends on the sounder code length M and chip period T_c: $0 \leq \tau_{rms} \leq M \cdot T_c$.

Hence, taking into account the set of these limits, for τ_{rms} and for CB, we can define a region of validity for the estimation of these two-channel parameters. This region is defined according to (4) and plotted in Fig. 6

$$\frac{\arccos(c)}{(2\pi \cdot \tau_{rms})} \leq CB \leq \frac{1}{T_c}, \quad 0 \leq \tau_{rms} \leq M \cdot T_c \tag{4}$$

All plots of Figs. 3–5 fall in the validity region defined in (4). We can also derive the minimum measurable value for CB that will take place when τ_{rms} reaches the maximum discernible delay, τ_{max}, as given in (5)

$$CB_{min} = \frac{\arccos(c)}{(2\pi \cdot M \cdot T_c)} \tag{5}$$

5 Analysis of the channel capacity

The estimated CBs values are important to study the applications that can be implemented in the 40 GHz

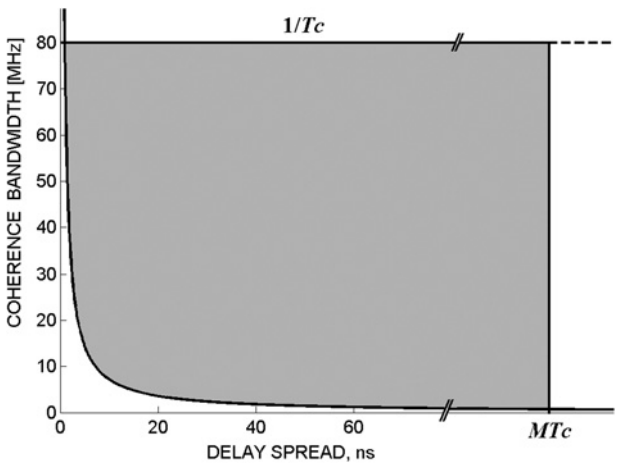

Fig. 6 *Validity region for CB and delay spread values*

frequency band. Typical modulations used in radio links to implement audio and data services are QPSK or 64-QAM, but video streaming applications or wireless internet demand multicarrier modulations such as OFDM 64-QAM. The theoretical BW necessary to transmit an uncoded QPSK or QAM signal is given by (6)

$$R_b = \frac{\log_2 M}{(1+\alpha)} \cdot \mathrm{BW}_{\mathrm{QPSK/QAM}} \tag{6}$$

where $\mathrm{BW}_{\mathrm{QPSK/QAM}}$ is the bandwidth necessary for transmitting a QPSK- or QAM-modulated signal; M is the number of symbols; and α is the roll-off factor (usually 15%).

If the variable $\mathrm{BW}_{\mathrm{QPSK/QAM}}$ in (5) is substituted by the $\mathrm{CB}_{0.9/0.5}$, the result is the binary rate that is possible to achieve while maintaining stable amplitude and phase modulation. In Table 4, we have summarised the maximum bit rates available for the above modulations. Calculations are based on (5) and the range values for $\mathrm{CB}_{0.9/0.5}$ given in Tables 1–4.

Bit rate values are larger for outdoor environments, with 64-QAM modulation and a correlation level of 0.5. In general, predicted bit rates are high, which should allow many broadband applications. Room-to-room videoconferencing needs a data rate between 64K bps and 2048 Mbps, and 36 Mbit/s is approximately the capacity needed for a DVB-S transport stream.

The SAMBA project from the EU ACTS programme [4, 5], obtained data rates of 41 Mbps using the OQPSK modulation, over a cell radius between 6 and 200 m at 40 GHz band. The MBS project [1] presented expectations of data rates up to 155 Mbps, at 40 and 60 GHz, for indoor and outdoor environments. In order to support a data rate of 155 Mbps, the required BW should be 155/4 = 38.75 MHz for the QPSK modulation case, and 2.42 MHz for 64-QAM. Those values are compatible with the CBs obtained in our measurements as indicated in Tables 1–4.

For the analysis of the 64-QAM OFDM case we have followed expressions (7 and 8)

$$R_{\mathrm{b,OFDM}} = N \cdot R_{\mathrm{b,64-QAM}} \tag{7}$$

$$N = \mathrm{CB}_{0.9/0.5}/\Delta f \tag{8}$$

Firstly we estimated the number of carriers N as the ratio given by a frequency slot equal to $\mathrm{CB}_{0.9/0.5}$ and a carrier separation $\Delta f = 0.5$ MHz. Then, the R_b for the OFDM results from multiplying the number of carriers N and the (gross) bit rate obtained for a single 64-QAM with a channel BW of Δf, that is 3 Mbps from (5) and $\alpha = 0$. In Table 4, the last column shows the values obtained for the 64-QAM OFDM case. The capacity has increased dramatically even for the outdoor–indoor case (NLOS).

We can predict the theoretical effect of the use of spatial diversity on the bit rate taking into account the results obtained in [24]. If an improvement of 5 dB is achieved for the fading, then it can be considered that the signal-to-noise ratio (SNR) increases by 5 dB, and consequently the bit rate R_b will achieve larger values. According to Shannon's expression for the channel capacity $C = R_\mathrm{b} = \mathrm{BW}\cdot\log_2(1+\mathrm{SNR})$, it is demonstrated that an upgrading factor ΔC given by (9) can be obtained if a spatial diversity system is used at the receiver end together with a maximal ratio combining (MRC) or equal gain combining (EGC) scheme for the same bandwidth BW and

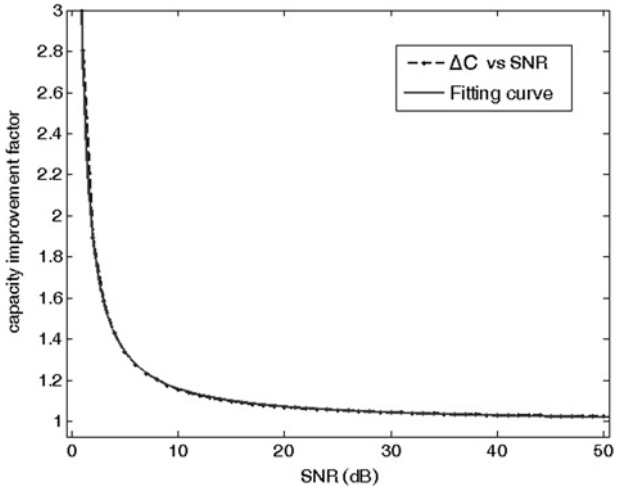

Fig. 7 *Channel capacity improvement factor as a function of SNR*

with diversity gain DG

$$\Delta C = \frac{C_{\mathrm{SNR+DG}}}{C_{\mathrm{SNR}}} = \frac{\log_2(1+\mathrm{SNR}+\mathrm{DG})}{\log_2(1+\mathrm{SNR})} \tag{9}$$

$$\Delta C \simeq \frac{\mathrm{DG}}{\mathrm{DG}+1} \cdot \frac{1}{\mathrm{SNR}} + 1 \tag{10}$$

where the SNR must be strictly positive. We have derived an approximation (10) for the theoretical expression of ΔC (9), as a function of the DG and SNR according to a fitting curve that follows the equation $a \cdot x^b + c$. In Fig. 7, we plot both expressions (9) and (10) for DG = 5 and SNR in the range [1, 50] dB. Note that ΔC tends to infinity if the SNR tends to zero, and it will tend to +1 for SNR values larger than +25 dB. The improvement experienced by the channel capacity for a SNR of +1 dB and DG = 5 would be 2.8.

6 Conclusions

We have presented a measurement campaign carried out to obtain wideband characterisation of the radio channel for the 40 GHz band. We have discussed the influence of environment, antenna pattern and polarisation on the channel parameters. Results obtained from the measurements augur well for the use of the 40 GHz band for broadband services with high bit rates.

The relation between CB and delay spread shows to be dependent on the measurement scenario and antenna polarisation. The measured values and derived τ_{rms}-CB relations have been found verify the theoretical restriction given in [15]. They are also included in the validity region defined as an extension of this boundary.

We have demonstrated theoretically hat further but simple improvements can be applied to increase channel capacities, such as spatial diversity and the use of multicarrier modulations (OFDM), but many other techniques, could also be considered such as coding, MIMO technologies and so on.

7 Acknowledgments

We are grateful for the support received from the People Program of 7th FrameWork Programme (2008 Marie Curie IOF Action). This work was supported in part by the Spanish Ministry of Science and Innovation under grant no. TEC2005-00330.

8 References

1 Mobile Broadband Systems (MBS) – Draft Final Report, ERO, November 1996
2 ACTS Project CRABS: Interactive broadband technology trials, Deliverable D4P4, 1999
3 IST EMBRACE Project 1999
4 Proceedings of the RACE Mobile Telecommunications Summit, European Commission, Cascais, Portugal, 22–24 November 1995
5 Fernandes, L.: 'Developing a system concept and technologies for mobile broadband communications', *IEEE Pers. Commun. Mag.*, 1995, **2**, (1), pp. 54–59
6 CEPT Decision ERC/DEC/(99)16: 'ERC decision of 1 June 1999 on the designation of the harmonised frequency band 40.5 to 43.5 GHz for the introduction of multimedia wireless systems (MWS), including multipoint video distribution systems (MVDS)', 1999
7 CEPT Recommendation CEPT/ERC/REC(01)-04: 'Recommended guidelines for the accommodation and assignment of multimedia wireless systems (MWS) in the frequency band 40.5–43.5 GHz', 2001
8 Muhi-Eldeen, Z., Ivrissimtzis, L.P., Al-Nuaimi, M.O.: 'Measurements and modelling of cellular interference in local point-to-multipoint distribution systems', *IET Microw. Antennas Propag.*, 2009, **3**, (2), pp. 250–259
9 Fernández, O., Jaramillo, R., Domingo, M., Valle, L., Torres, R.P.: 'Characterization and modeling of BFWA channels in outdoor–indoor environments', *IEEE Antennas Wirel. Propag. Lett.*, 2007, **6**, pp. 236–239
10 Combeau, P., Aveneau, L., Vauzelle, R., Pousset, Y.: 'Efficient 2-D ray-tracing method for narrow and wideband channel characterisation in microcellular configurations', *IEE Proc. Microw. Antennas Propag.*, 2006, **153**, (6), pp. 502–509
11 Bello, P.A.: 'Characterization of randomly time-variant linear channels', *IEEE Trans. Commun. Syst.*, 1963, **11**, (4), pp. 360–393
12 Amoroso, F.: 'Use of DS/SS signaling to mitigate Rayleigh fading in a dense scatterer environment', *IEEE Pers. Commun.*, 1996, **3**, (2), pp. 52–61
13 Sklar, B.: 'Rayleigh fading channels in mobile digital communication systems. Part II: mitigation', *IEEE Commun. Mag.*, 1997, **35**, (7), pp. 102–109
14 Delangre, O., De Doncker, P., Lienard, M., Degauque, P.: 'Delay spread and coherence bandwidth in reverberation chamber', *Electron. Lett.*, 2008, **44**, (8), pp. 328–329
15 Fleury, B.H.: 'An uncertainty relation for WSS processes and its application to WSSUS systems', *IEEE Trans. Commun.*, 1996, **44**, (12), pp. 1632–1634
16 Parsons, J.D., Demery, D.A., Turkmani, A.M.D.: 'Sounding techniques for wideband mobile radio channels: a review', *IEE Proc. I Commun. Speech Vis.*, 1991, **138**, pp. 437–446
17 Bohdanovicz, A.: 'Wideband indoor and outdoor radio channel measurements'. UbiCom-TechnicalReport/2000/2, Delft University of Technology, 2000
18 Venkatesh, S., Buehrer, R.M.: 'Non-line-of-sight identification in ultra-wideband systems based on received signal statistics', *IET Microw. Antennas Propag.*, 2007, **1**, (6), pp. 1120–1130
19 Malik, W.Q., Allen, B., Edwards, D.J.: 'Bandwidth-dependent modelling of smallscale fade depth in wireless channels', *IET Microw. Antennas Propag.*, 2008, **2**, (6), pp. 519–528
20 Dinís, M., García, J., Monteiro, V., Oliveira, N.: 'Millimetre-wave channel impulse response experimental evaluation and relation between delay spread and channel coherence bandwidth'. 13th IEEE Int. Symp. on Personal, Indoor and Mobile Radio Communications, Lisboa, Portugal, 2002, vol. 5, pp. 2292–2296
21 Correia, L.M., Prassad, R.: 'An overview of wireless broadband communications', *IEEE Commun. Mag.*, 1997, **35**, (1), pp. 28–33
22 Larbi, T., Denidni, T.A.: 'Ultrawideband measurements for wireless indoor communications systems at 37.2 GHz', *IET Electron. Lett.*, 2002, **38**, pp. 1477–1479
23 Xu, H., Rappaport, T.S., Boyle, R.J., Schaffner, J.H.: '38-GHz wide-band point-to-multipoint measurements under different weather conditions', *IEEE Commun. Lett.*, 2000, **4**, (1), pp. 7–8
24 García Sánchez, M., Vázquez Alejos, A., Cuinas, I.: 'Space diversity performance in indoor radio channels at 40 GHz', *IET Electron. Lett.*, 2008, **44**, (20), pp. 1209–1210